Journal of Alloys and Compounds, 544 (2012) 73-81

http://dx.doi.org/10.1016/j.jallcom.2012.08.002

Extension of the classical theory of crystallization to non-isothermal regimes: Application to nanocrystallization processes

J. S. Blázquez[a]*, J. M. Borrego[a], C. F. Conde[a], A. Conde[a], S. Lozano-Pérez[b]

[a]*Departamento de Física de la Materia Condensada. Instituto de Ciencia de Materiales, CSIC Universidad de Sevilla. Apartado 1065, 41080-Sevilla, Spain.*

[b]*Department of Materials, University of Oxford, Parks Road, Oxford, OX1 3PH, UK*

Abstract

The non-isothermal kinetics of primary crystallization processes is studied from numerically generated curves and their predictions have been tested in several nanocrystallization processes. Single processes and transformations involving two overlapped processes in a non-isothermal regime have been generated and deviations from isokinetic behavior are found when the overlapped processes have different activation energies. In the case of overlapped processes competing for the same type of atoms, the heating rate dependence of the obtained Avrami exponent can supply information on the activation energies of each individual processes. The application to experimental data of nanocrystallization processes is consistent with a limited growth approximation. In the case of preexisting crystallites in the as-cast samples, predictions on the heating rate dependence of the obtained Avrami exponents of multiple processes have been confirmed.

Keywords: Johnson-Mehl-Avrami-Kolmogorov equation, crystallization, phase transformation kinetics, nanocrystalline microstructure.

*Corresponding author: J. S. Blázquez
Phone: (34) 95 455 60 29
Fax: (34) 95 461 20 97
E-mail: jsebas@us.es;

Journal of Alloys and Compounds, 544 (2012) 73-81

http://dx.doi.org/10.1016/j.jallcom.2012.08.002

1. Introduction

The study of the devitrification kinetics in glassy metals has received attention since their discovery [1-3]. The application of the classical theory of crystallization (based on nucleation and growth processes) to this process was also early adapted [2, 3]. This theory was developed independently by Kolmogorov [4, 5], Jhonson and Mehl [6] and Avrami [7] (JMAK theory) in the late 30's of the last century to be applied to isothermal polymorphic transformations. However, it can be appropriately extended to transformations implying compositional changes [8, 9] and to non-isothermal processes [10-19].

In this work, a direct extension of the classical theory of isothermal crystallization to non-isothermal processes, previously proposed by the authors [16], is revised in order to solve deviations observed for low transformed fractions. In the frame of this approach, the kinetic analysis of the primary crystallization of several metallic glasses including the development of single or multiple phases is evaluated. Nanocrystallization processes fulfill most of the five postulates of Kolmogorov (listed in Ref. [5]). In the case of nanocrystallization processes, the crystallites can be considered spherical (isotropic growth) and non-random nucleation is claimed to occur (due to non-homogeneity of the matrix [20], nucleation enhancement by Cu clustering phenomena [21-23] or formation of agglomerates in Hitperm alloys [24]). However, random nucleation can be assumed as an approximation for a global view of the transformation.

2. Kinetics of crystallization

Journal of Alloys and Compounds, 544 (2012) 73-81

http://dx.doi.org/10.1016/j.jallcom.2012.08.002

2.1 Isothermal processes

In JMAK theory, the extended transformed fraction, X^* [5] corresponds to the fraction of the system that should be transformed if any growing crystal could freely grow without impinging with another growing crystal (i.e. if no geometrical impingement occurred). It is obtained from the nucleation rate, $I=dN/dt$ (N being the number of nuclei formed per unit volume, and t, the time), and the rate of linear growth, $G=dR/dt$ (R being the average radius of the crystals). For isotropic growth in three dimensions:

$$X^* = \frac{4\pi}{3}\int_0^t I(t')\left(\int_{t'}^t G(\tau)\,d\tau\right)^3 dt' \tag{1}$$

where crystals are considered to be spherical. Assuming power laws for nucleation rate $I=I_0 \cdot t^b$ and linear growth $G=G_0 \cdot t^a$, results:

$$X^* = \frac{4\pi}{3}\frac{I_0 G_0^{\,3}}{C} t^{3(a+1)+b+1} = Kt^n = (kt)^n \tag{2}$$

with C a constant, $k=K^{1/n}$, the frequency factor, and n, the Avrami exponent. The value of this exponent can be decomposed as $n=n_I+3 \cdot n_G$, where $n_I=1+b$ corresponds to nucleation (with a nucleation rate constant if b=0 (n_I=1), increasing $I(t)$ if b>0 and decreasing $I(t)$ if b<0); and $n_G=a$+1 corresponds to growth (n_G=1/2, for diffusion controlled growth, $G=G_0/t^{1/2}$, and n_G=1 for interface controlled growth, $G=G_0$).

The relationship between X^* and the actual transformed fraction, X, is obtained considering a statistical geometrical impingement:

Journal of Alloys and Compounds, 544 (2012) 73-81

http://dx.doi.org/10.1016/j.jallcom.2012.08.002

$$\frac{dX}{dX*} = 1 - X \tag{3}$$

The JMAK equation results when Eq. (2) and (3) are combined:

$$X = 1 - \exp\left(-(kt)^n\right) \tag{4}$$

2.2 Extension to non-isothermal processes

Nakamura et al. [25] proposed a general expression of the transformation equation to extend JMAK equation to non-isothermal processes, which for a constant heating rate β results:

$$X = 1 - \exp\left\{-\left(1/\beta^n\right)\left[\int_{To}^{T} k(T)dT\right]^n\right\} \tag{5}$$

where T is the temperature, T_O is the onset temperature and $k(T)=k_0\exp(-Q/k_BT)$ is a temperature dependent frequency factor, which is assumed to follow an Arrhenius law with Q, the activation energy, and k_B, the Boltzmann constant.

Later on, some of the present authors simplified Nakamura's expression considering the following approximation [16]:

$$k'_0 \exp\left[-Q/k_BT\right](T - T_o') = \int_{To}^{T} k(T)dT \tag{6}$$

Journal of Alloys and Compounds, 544 (2012) 73-81

http://dx.doi.org/10.1016/j.jallcom.2012.08.002

In previous works [16, 26-30], it was implicitly assumed $T_O' = T_O$ (the onset temperature of the process). However, a deeper insight into this relationship is required to appreciate the effect of T_O' on the estimated values.

If we divide the two terms of equation (6) by $k(T)$ we obtain a function $A(T)$:

$$\frac{k'_0}{k_0}(T - T_o') = \frac{\beta \int_0^t k(T)dt}{k(T)} = A(T) \tag{7}$$

which, according to Eq. (6), can be approximated to a straight line for a certain temperature range and, thus:

$$\frac{dA(T)}{dT} = \frac{k'_0}{k_0} = D(T) \tag{8}$$

The value of T_O' which leads to the best fitting depends on the value of the temperature T at which the approximation will be performed:

$$T_o' = T - \frac{A(T)}{D(T)} \tag{9}$$

Figure 1a shows the value of T_O' as a function of the temperature, T, at which the approximation of Nakamura's expression is performed for activation energies in the range 0.5-10 eV. Except for Q<2 eV, a very good linear behavior can be found in a wide temperature range (from ~100 K to >1000 K), which extends far beyond the temperature range of interest for practical uses in the analysis of devitrification processes of amorphous alloys. As an example, for Q=4 eV (typical value for primary

crystallization processes of Fe-based amorphous alloys [3]) the fitting gives T_O'=[0.48993(2)·T+2.43(1)] K.

As Q changes from 3 to 10 eV, the slope of the straight line increases 2 % and the value of the intercept with the Y-axis decreases from ~3 K to 0.3 K. These results allow us to propose an approximated value of T_O' for practical applications:

$$T_O' = T_P/2 \quad (10)$$

where T_P is the crystallization peak temperature and thus, the temperature around which it is found the thermal range of interest to perform the simplification of Nakamura's expression. It is worth mentioning that the present result is independent of the values of β, k_0 and k_0'. Moreover, as this approximation affects X*, it is also independent of whether the kinetics of transformation follows JMAK equation or an expression considering a generalized impingement parameter [31, 32].

In order to appreciate the goodness of the proposed approximation, figure 1b shows the two terms of Eq. (7) using $T_O'=T_P/2$ along with the corresponding curve of the transformation rate generated using Nakamura's equation (k_0=10^{25} s^{-1}, n=4, Q=4 eV, β=10 K/min) as will be explained below. Only one free parameter, k_0'/k_0, has been used to fit $A(T)$ function in the temperature range from 730 K to 760 K resulting k_0'/k_0=5.314(3).

3. Results. Validity of the approximation using numerically generated curves

3.1 Crystallization processes implying the formation of a single phase

Journal of Alloys and Compounds, 544 (2012) 73-81

http://dx.doi.org/10.1016/j.jallcom.2012.08.002

In order to appreciate the effect of T_O' on the Avrami exponent obtained applying the approximation of a direct extension to non-isothermal processes of Avrami equation, a systematic procedure was followed. Kinetic curves of $X(t)$ were generated using Eq. (5) for different values of β (from 10 to 60 K/min), Q and n; and Kissinger method [33] was applied to recalculate the activation energy of the numerically generated curves. As an example, for Q=4 eV, Kissinger analysis yields Q'=3.9965 eV for n=1 (regression coefficient, $r^2 > 0.9998$), with a better linear fitting as n increases. Afterwards, the corresponding curves were analyzed and local Avrami exponents were recalculated applying the relationship:

$$n(X) = \frac{d\left(Ln\left[-Ln(1-X)\right]\right)}{d\left(Ln\left[(T-T_O')/\beta\right]\right)}\left\{1+\frac{Q'}{k_B T}\left(1-\frac{T_O'}{T}\right)\right\}^{-1} \qquad (11)$$

derived from Eq.(18) of Ref. [16].

Figure 2 shows the results obtained for a numerically generated process with parameters n=1, Q=4 eV, $k_0=10^{25}$ s^{-1} and β=10, 20, 30, 40, 50 and 60 K/min, respectively. Different values of T_O' were considered: a) the onset temperature, T_O, estimated as the interception with the baseline of the steepest slope of dX/dt plot; b) a temperature below the onset temperature at which there is no appreciable deviation of the dX/dt signal from the baseline; c) the value suggested by the above mentioned discussion, $T_P/2$; d) room temperature; and e) 0 K.

As an example, some of these temperatures are indicated in the inset of figure 2 on a dX/dt plot generated using Nakamura's kinetic equation at 10 K/min.

Journal of Alloys and Compounds, 544 (2012) 73-81

http://dx.doi.org/10.1016/j.jallcom.2012.08.002

Deviations from the actual value (n=1 in the example shown) are important for low values of transformed fractions when $T_O'=T_O$ is chosen. Good results are obtained (with an error below 0.1%) for $T_O'=T_P/2$. The use of lower values of T_O' does not significantly affect the resulting Avrami exponent, although its value is slightly overestimated.

3.2 Crystallization processes implying the formation of multiple phases

Frequently, the first DSC peak of a devitrification process corresponds to several overlapped transformations. In fact, several crystalline phases can be developed and they can overlap in time (isothermal regimes) or temperature (non-isothermal regimes). In order to study the effect of applying the proposed non-isothermal analysis to such transformations, the simplest case of two independent processes is considered.

As a first approximation, the transformation curves can be numerically generated using Nakamura's equation in the following way:

$$X = f\left(1-\exp\left\{-\left[\int_0^t k_1(T)dt\right]^{n_1}\right\}\right)+(1-f)\left(1-\exp\left\{-\left[\int_0^t k_2(T)dt\right]^{n_2}\right\}\right) \qquad (12)$$

where f is the fraction of phase 1at the end of the crystallization process. The kinetics of formation of phase 1 is characterized by the parameters n_1, Q_1 and k_{01} (Avrami exponent, activation energy, and frequency factor, respectively), being n_2, Q_2, k_{02} the corresponding set of phase 2. This construction assures that the fraction of each phase at the end of the whole process (f and 1-f, respectively) is independent of β.

Journal of Alloys and Compounds, 544 (2012) 73-81

http://dx.doi.org/10.1016/j.jallcom.2012.08.002

An example of the *dX/dt* functions generated using Eq. (12) for two different values of β and typical temperatures for primary crystallization of amorphous alloys are shown in figure 3a (the fractions ascribed to each individual transformation are also shown).

Kissinger method was applied to calculate the average activation energy, $<Q>$, of the whole process. Figure 4 shows three examples of $<Q>$ as a function of the final fraction of phase 1. It can be observed that the behavior of $<Q>$ is far from being linear with *f*. These values of $<Q>$ have been used to apply the direct extension to non-isothermal processes of the JMAK equation using Eq. (11). Results are shown in figure 3b. It is worth noticing that although isokinetic behavior would be expected, it is not reproduced unless $Q_1=Q_2$. For a given *X*, there is no clear dependence of the Avrami exponent with β. In fact, an increasing or decreasing *n* with β can be obtained for the same set of values n_1, n_2, Q_1, Q_2 depending on the frequency factors k_{01} and k_{02} used. In fact, completely separated peaks can be obtained tailoring these frequency factors. Therefore, it can be concluded that, for the processes generated using Eq.(12), non-isokinetic deviations are an artifact.

Expression (12) implicitly assumes that each process has a fraction of the total volume *V* of the sample (fV and $(1-f)V$, respectively) only accessible to each corresponding phase and that is not accessible to the other phase. In order to overcome this limitation, we can use the idea of the extended volume, which is not affected by the remaining untransformed fraction. Thus, a total extended volume fraction can be defined as the sum of the extended transformed fractions of each process: $X^*=X_1^*+X_2^*$ (as also proposed in [34]). Thus,

Journal of Alloys and Compounds, 544 (2012) 73-81

http://dx.doi.org/10.1016/j.jallcom.2012.08.002

$$X = 1 - \exp\left\{ -\left(\left[\int_0^t k_1(T)dt \right]^{n_1} + \left[\int_0^t k_2(T)dt \right]^{n_2} \right) \right\} \quad (13)$$

If a transformation involves the production of two different phases, with different composition, Eq. (12) could be more appropriate than Eq. (13) if it is assumed that the different processes do not compete for the same kind of atoms. Therefore, the volume ascribed to each atom (allowing it to diffuse through the sample) would correspond to only one process. However, if different processes compete for the same atoms, Eq. (13) will be more appropriate to describe the total transformed fraction. In both cases, the simplification that there is no dependency of the kinetic parameters (activation energy, Avrami exponent or frequency factor) of one phase on the degree of transformation of the second one was assumed.

Figure 5a-c shows *dX/dt* functions generated using equation (13) for two different β (10 and 60 K/min) and different values of Avrami exponents, activation energies and frequency factors for each individual process. This figure also shows the contributions ascribed to each individual process, calculated after separating the contribution of each phase to the variation of the extended transformed fraction:

$$\frac{1}{1-X}\frac{dX_i}{dt} = \frac{dX_i^*}{dt} \quad (14)$$

where the sub index i=1, 2 identifies each individual process. It should be mentioned that the fraction of each phase at the end of the process depends on the heating rate unless the activation energies were equal. This result contrasts with that of the previous generated multiple process assuming addition of actual transformed fractions. In fact, as heating rate increases, the process with the highest activation energy is delayed in

Journal of Alloys and Compounds, 544 (2012) 73-81

http://dx.doi.org/10.1016/j.jallcom.2012.08.002

temperature and thus the remaining untransformed volume, available for its development, is reduced due to the progress of the process with lower *Q*. Therefore, non-isokinetic behavior must be expected. Moreover, using this approach, it is not possible to obtain separated peaks, discarding those cases in which overlapped peaks can be experimentally separated by changing thermal treatment.

Figure 5d-f shows the Avrami exponents obtained from the analysis of the multiple processes generated by addition of the extended transformed fractions (Eq. (13)). It can be observed that, for given activation energies, the tailoring of frequency factors can lead to a negligible contribution of one of the two processes. Only in these cases, which actually correspond to single processes, or when $Q_1=Q_2$, isokinetic behavior is reproduced. It is noteworthy that when the highest Avrami exponent corresponds to the process with the highest *Q* value, the Avrami exponent obtained from the analysis, increases with the heating rate but in the case for which the highest Avrami exponent corresponds to the lowest *Q* value process, the Avrami exponent obtained decreases as β increases.

4. Discussion. Application to experimental curves

Ribbon samples of $Fe_{60}Co_{18}Nb_6B_{16}$ alloy and $Fe_{65.5}Cr_{4-x}Mo_{4-y}Cu_{x+y}Ga_4P_{12}C_5B_{5.5}$ alloy series (x=0, 1; y=0, 0.5, 1) were obtained by melt-spinning technique. Differential scanning calorimetry (DSC) scans were performed in a Perkin-Elmer DSC7. Transmission electron microscopy (TEM) experiments were performed in a Philips CM200 at 200 kV and high resolution electron microscopy (HREM) was performed in a Jeol JEM3000F operated at 297 kV.

Journal of Alloys and Compounds, 544 (2012) 73-81

http://dx.doi.org/10.1016/j.jallcom.2012.08.002

4.1 $Fe_{60}Co_{18}Nb_6B_{16}$ (single phase crystallization)

Figure 6 shows the local Avrami exponent obtained for $Fe_{60}Co_{18}Nb_6B_{16}$ amorphous alloy ascribed to the primary crystallization (corresponding heat flow curve is shown in the inset) using Eq. (11) with different values of T_O'. By comparing the results after setting $T_O'=T_P/2$ with the previously published ones, using $T_O'=T_O$, [16], deviations are found only for low crystalline fractions. The average value for the whole range of transformed fractions, $\langle n \rangle \sim 0.9$, concurs with the Avrami exponent obtained from Gao-Wang method [35]. The agreement with those values obtained from Ozawa method [16]remains in this study. In fact, changes in T_O' have no influence for high transformed fractions.

At very low X, n reaches values above 2.5 (constant nucleation rate and diffusion controlled growth). These values could be understood in the frame of classical JMAK theory as due to both: a) an enhanced nucleation rate ($n_I>1$, which may be associated to the presence of crystalline agglomerates [36], as shown in figure 7) and/or b) a transient interface controlled growth ($n_G=3$) as Clavaguera-Mora et al. [3] used to describe the initial stages of primary crystallization processes.

However, it must be taken into account that those values corresponding to $X<0.1$ are very sensitive to baseline selection. As crystallization progresses, Avrami exponent decreases to values below 1, indicating a strong impingement in the growth process and a decreasing nucleation rate, which has been simulated with Cellular Automata in the frame of an instantaneous growth approximation [36]. The extension of this latter model to a limited growth approximation yielded very similar values of the local Avrami

exponents (decreasing from 4 to below 1) [37] as those found here. This limited growth process can be understood as a simplification of the kinetic description of Clavaguera-Mora et al. [3] including an initial transient interface controlled growth (n_G=3) followed by a diffusion controlled growth affected by soft impingement. In the limited growth approximation, only the transient interface controlled growth is considered. In the present case, we can consider two different processes competing for the same kind of atoms (described by Eq. (13)), resulting in a fraction of the crystals that will grow, whereas the rest of crystals will remain blocked. At the final stages of the transformation the fraction of crystals growing will be very small and thus, the progress of the transformation should be limited to the nucleation phenomena. At this stage we can proceed as follows:

$$X^* = \left(\frac{N_G}{N_G + N_B}\right)\left[\int_0^t k(T)dt\right]^{n_G+n_I} + \left(\frac{N_B}{N_G + N_B}\right)\left[\int_0^t k(T)dt\right]^{n_I} \sim \left[\frac{1}{\beta}\int_{T_O}^{T} k(T)dT\right]^{n_I} \quad (15)$$

where N_G is the number of crystal growing and N_B is the fraction of crystals blocked. For sufficiently large values of time, $N_G << N_B$. The application of the approximation developed in the present paper (Eq. (11)) to Eq. (15), results:

$$Ln\left(-Ln\left(1-X\right)\right) = -n_I Ln\left(\beta\right) + n_I Ln\left(k_0'\right) - \frac{n_I Q}{k_B T} + n_I Ln\left(T - \frac{T_P}{2}\right) \quad (16)$$

This expression, analogous to that developed by Ozawa [12], could be used in the present context to obtain the nucleation contribution to the Avrami exponent, n_I, at a fixed temperature at which the growth contribution is negligible. In the case of the studied $Fe_{60}Co_{18}Nb_6B_{16}$ alloy, the average slope of the different linear fittings, in the

temperature range from 825 to 895 K with β from 2.5 to 80 K/min (figure 8a), yields n_I=0.211±0.006.

The intercept *y(T)* with the Y-axis is temperature dependent:

$$y(T) = n_I Ln\left(T - \frac{T_P}{2}\right) + n_I Ln(k_0') - \frac{n_I Q}{k_B T} \quad (17)$$

and neglecting the value of the first logarithmic term with respect to that proportional to 1/*T*, a linear fitting of *y(T)* vs. 1/*T* (shown in figure 8b) would lead to a slope $-n_I Q/k_B$, from which Q=4.3±0.3 eV is obtained (in good agreement with the values obtained using other methods [16]). However, this activation energy might correspond to high transformed fractions whereas those reported in Ref. [16] correspond to the transformed fraction at the peak temperature. Moreover, a value of Q=3.6±0.3 eV was found from the temperature dependence of the induction time in isothermal experiments [38]. This fact points to an almost constant activation energy along the transformation process.

At the initial stage of the nanocrystallization, the fraction of crystallites blocked should be negligible and the Avrami exponent could be expressed by $n=n_I+3\cdot n_G$. Assuming n_I~0.2 and n_G=1 (interface controlled), the value of n=3.2 is coherent with the observed values in figure 6 for very low transformed fractions. The very low values of n_I could be ascribed to deviations from random nucleation.

Other possible kinetic analysis could be performed in the frame of the general impingement parameter [31]. However, even in the extreme case of Austin-Rickett kinetic equation, the analysis brings out values of n=0.65±0.12, reporting no advantage in the interpretation with respect to the above mentioned analysis on the frame of limited growth.

Journal of Alloys and Compounds, 544 (2012) 73-81

http://dx.doi.org/10.1016/j.jallcom.2012.08.002

5.2 $Fe_{65.5}Cr_{4-x}Mo_{4-y}Cu_{x+y}Ga_4P_{12}C_5B_{5.5}$ (crystallization of multiple phases)

The direct extension of JMAK equation to non-isothermal processes has also been applied to the bulk amorphous compositional series $Fe_{65.5}Cr_{4-x}Mo_{4-y}Cu_{x+y}Ga_4P_{12}C_5B_{5.5}$ (x=0, 1; y=0, 0.5, 1). The parent alloy (x=0, y=0) exhibits a large supercooled liquid region (>60 K) which decreases after Cu addition [39]. Cu addition yields a primary crystallization process consisting in the formation of nanocrystalline α-Fe(Ga) phase, whereas Cu-free alloy developed several phases after the first transformation stage [39]. Figure 9a-d shows the DSC plots of the different studied alloys at different heating rates and figure 9e-h shows the corresponding local Avrami exponents obtained from application of Eq. (11).

It can be noticed that the curves for Cu-free alloy are clearly non isokinetic, in agreement with the multiple transformation character of the primary crystallization of this alloy. In the case of the Cu containing alloys, isokinetic behavior is better fulfilled, although some deviation could be observed, particularly for the alloys with 1 and 2 at. % of Cu. In fact, TEM studies on as-cast samples of these alloys showed the presence of crystallites of α-Fe(Ga) phase, which implies the existence of two competitive processes in the transformation: growth of the preexisting crystals and nucleation and growth of new α-Fe(Ga) crystallites. Figure 10 shows TEM images of both, as-cast samples and samples heated up to the end of the first transformation stage.

In the case of alloys with 0.5 at. % of Cu no preexisting crystals were detected and, consequently, a single process is expected. Nanocrystallization kinetics of this alloy can be interpreted in the same way as done for the previously discussed

Journal of Alloys and Compounds, 544 (2012) 73-81

http://dx.doi.org/10.1016/j.jallcom.2012.08.002

$Fe_{60}Co_{18}Nb_6B_{16}$ alloy. In the frame of the limited growth approach, the Avrami exponents at the end of the process can be ascribed to nucleation phenomena with n_I~1. At low crystalline volume fractions, the expected values should be ascribed to transient interface controlled growth (affecting to all the crystal formed) plus nucleation n=4.

In the case of the alloys with 1 and 2 at. % of Cu, the initial values of n are not as high as those found for the alloy with 0.5 at. % of Cu. Unlike for this alloy, at the initial stages of crystallization n values clearly depart from isokinetic behavior for the alloys with higher Cu content. This might be due to the two different processes occurring for these alloys (growth of preexisting crystals and nucleation and limited growth of the new formed crystals). At the very beginning of the transformation, the main process is the growth of the preexisting crystals as the transformed fraction ascribed to nucleation and growth of the new crystallites is negligible. This should allow us to approximate the Avrami exponent at the initial stages of transformation to the type of growth of these preexisting crystals. At X~0.05 (fraction at which n~4 for the alloy with 0.5 at. % of Cu), n~1.5-2.5 for the alloy with 1 at. % of Cu and n~2.5-3.5 for the alloy with 2 at. % of Cu, increasing as β increases.

Deviations from isokinetic behavior in these two alloys (1 and 2 at. % of Cu) yields to higher Avrami exponents as β increases. As it has been explained before, this feature has been above mentioned using Nakamura's equations if the process with the highest Avrami exponent is also the process with the highest activation energy. In the present case, a lower Avrami exponent must correspond to the process of growth of preexisting crystals, rather than to the process involving nucleation and growth of new crystallites. Therefore, the observed β dependence of n indicates a lower activation

energy for the process with the lower Avrami exponent: i.e. the growth of the crystals already present in the as-cast samples.

This is in agreement with the lower enthalpy ascribed to the first transformation stage (the one studied here) in the case of the alloys with 1 and 2 at. % of Cu (12.1±0.2 kJ/kg and 11.0±0.2 kJ/kg, respectively) than for the alloy with 0.5 at. % (23.5±0.2 kJ/kg). A lower enthalpy per transformed volume implies lower activation energy of the process assuming most of the kinetic parameters involved in both processes must be similar. The crystalline fraction at the end of the nanocrystallization process measured by XRD is similar for the alloys with Cu of the studied series [39] and, therefore, a lower enthalpy might correspond to those compositions with crystalline phase already present in the as-cast sample. However, the large difference (~50 %) in enthalpy cannot be attributed only to the little amount of crystallites already formed in the as-cast sample. In fact, for the alloy with 2 at. % of Cu, the preexisting crystals grow from 26 to 40 nm and this implies that the initial crystalline fraction is only ~25 % of the crystalline fraction due to the growth of the preexisting crystallites and, consequently, much lower values with respect to the whole crystalline fraction.

Conclusions

The approach to directly extend the Avrami equation to non-isothermal regimes previously reported is revised in order to solve some deviations of the Avrami exponents observed for very low transformed fractions.

A final expression of the local Avrami exponent is reported as:

Journal of Alloys and Compounds, 544 (2012) 73-81

http://dx.doi.org/10.1016/j.jallcom.2012.08.002

$$n(X) = \frac{d\left(Ln\left[-Ln(1-X)\right]\right)}{d\left(Ln\left[\left(T-\frac{T_P}{2}\right)/\beta\right]\right)}\left\{1+\frac{Q}{k_B T}\left(1-\frac{T_P}{2T}\right)\right\}^{-1}$$

where X is the transformed fraction; β, the heating rate; Q, the activation energy; T the temperature and T_P the peak temperature.

Effects on the obtained Avrami exponents by applying this approach to single processes and transformations involving two overlapped processes (in both cases, independent processes and competing processes) are discussed and deviations are found from isokinetic behavior when the overlapped processes have different activation energies.

In the case of processes competing for the same type of atoms, the Avrami exponent, n, for a given value of transformed fraction, increases as β increases if the activation energy is higher for the process with the highest Avrami exponent. The n value decreases if the activation energy is higher for the process with the lowest Avrami exponent.

Applications to experimental data are consistent with a limited growth approximation. In the case of preexisting crystallites in the as-cast samples, experimental results confirm the predictions on the β dependence of the obtained Avrami exponents of multiple processes.

Acknowledgements: This work was supported by the Spanish Ministry of Science and Innovation (MICINN) and EU FEDER (project MAT2010-20537) and the PAI of the

Journal of Alloys and Compounds, 544 (2012) 73-81

http://dx.doi.org/10.1016/j.jallcom.2012.08.002

Regional Government of Andalucía (project P10-FQM-6462). Some TEM investigations were supported by the IP3 project of the 6th Framework Programme of the European Commission: ESTEEM Contract number 026019.

References

[1] P. Duwez, R.C. Crewdson, R.H. Willens, AMORPHOUS PHASE IN PD-SI ALLOYS, Jom-Journal of Metals, 16 (1964) 92-&.
[2] D.R. Uhlmann, A kinetic treatment of glass formation, Journal of Non-Crystalline Solids, 7 (1972) 12.
[3] M.T. Clavaguera-Mora, N. Clavaguera, D. Crespo, T. Pradell, Crystallisation kinetics and microstructure development in metallic systems, Progress in Materials Science, 47 (2002) 559-619.
[4] A.N. Kolmogorov, Static theory of metals cristallization, Bull Acad Sci USSR, Phys Ser, 1 (1938) 5.
[5] A.A. Burbelko, E. Fras, W. Kapturkiewicz, About Kolmogorov's statistical theory of phase transformation, Materials Science and Engineering A-Structural Materials Properties Microstructure and Processing, 413 (2005) 429-434.
[6] W.A. Johnson, R.F. Mehl, Reaction Kinetics in Processes of Nucleation and Growth (Reprinted from Transactions of the American Institute of Mining & Metallurgical Engineers, vol 135, pg 416, 1939), Metallurgical and Materials Transactions a-Physical Metallurgy and Materials Science, 41A (2010) 2713-2775.
[7] M. Avrami, Kinetics of phase change I - General theory, Journal of Chemical Physics, 7 (1939) 1103-1112.
[8] P. Bruna, D. Crespo, R. Gonzalez-Cinca, E. Pineda, On the validity of Avrami formalism in primary crystallization, Journal of Applied Physics, 100 (2006) 054907.
[9] J.S. Blazquez, M. Millan, C.F. Conde, A. Conde, Nucleation rate and nanocrystallization of Co-60-(Fe, Mn)(18)-Nb-6-B-16 amorphous alloys in the frame of instantaneous growth approximation, Journal of Alloys and Compounds, 505 (2010) 91-95.
[10] K. Nakamura, K. Katayama, T. Amano, SOME ASPECTS OF NONISOTHERMAL CRYSTALLIZATION OF POLYMERS .2. CONSIDERATION OF ISOKINETIC CONDITION, Journal of Applied Polymer Science, 17 (1973) 1031-1041.
[11] T.P. Prasad, S.B. Kanungo, H.S. Ray, NONISOTHERMAL KINETICS - SOME MERITS AND LIMITATIONS, Thermochimica Acta, 203 (1992) 503-514.
[12] T. Ozawa, KINETICS OF NON-ISOTHERMAL CRYSTALLIZATION, Polymer, 12 (1971) 150-158.
[13] V. Erukhimovitch, J. Baram, A model for non-isothermal crystallization kinetics, Journal of Non-Crystalline Solids, 208 (1996) 288-293.
[14] M.J. Starink, A.M. Zahra, Kinetics of isothermal and non-isothermal precipitation in an Al-6 at% Si alloy, Philosophical Magazine a-Physics of Condensed Matter Structure Defects and Mechanical Properties, 77 (1998) 187-199.
[15] A.T.W. Kempen, F. Sommer, E.J. Mittemeijer, Determination and interpretation of isothermal and non-isothermal transformation kinetics; the effective activation energies in terms of nucleation and growth, Journal of Materials Science, 37 (2002) 1321-1332.
[16] J.S. Blazquez, C.F. Conde, A. Conde, Non-isothermal approach to isokinetic crystallization processes: Application to the nanocrystallization of HITPERM alloys, Acta Materialia, 53 (2005) 2305-2311.

[17] J. Farjas, P. Roura, Modification of the Kolmogorov-Johnson-Mehl-Avrami rate equation for non-isothermal experiments and its analytical solution, Acta Materialia, 54 (2006) 5573-5579.
[18] H.C. Kou, J. Wang, B. Tang, X.F. Gu, R. Hu, J.S. Li, L. Zhou, Effect of the kinetic model on parameter distortions in non-isothermal transformations, Journal of Alloys and Compounds, 479 (2009) L22-L25.
[19] J. Torrens-Serra, P. Bruna, S. Roth, J. Rodriguez-Viejo, M.T. Clavaguera-Mora, Effect of minor Co additions on the crystallization and magnetic properties of Fe(Co)NbBCu alloys, Journal of Alloys and Compounds, 496 (2010) 202-207.
[20] E. Pineda, T. Pradell, D. Crespo, Non-random nucleation and the Avrami kinetics, Philosophical Magazine a-Physics of Condensed Matter Structure Defects and Mechanical Properties, 82 (2002) 107-121.
[21] M. Matsuura, M. Sakurai, S.H. Kim, A.P. Tsai, A. Inoue, K. Suzuki, On the role of small additives for nanocrystalline formation from amorphous matrix, Materials Science and Engineering a-Structural Materials Properties Microstructure and Processing, 217 (1996) 397-400.
[22] Y. Zhang, P.J. Warren, A. Cerezo, Effect of Cu addition on nanocrystallisation of Al-Ni-Sm amorphous alloy, Materials Science and Engineering a-Structural Materials Properties Microstructure and Processing, 327 (2002) 109-115.
[23] Y. Zhang, J.S. Blazquez, A. Conde, P.J. Warren, A. Cerezo, Partitioning of Co during crystallisation of Fe-Co-Nb-B(-Cu) amorphous alloys, Materials Science and Engineering a-Structural Materials Properties Microstructure and Processing, 353 (2003) 158-163.
[24] J.S. Blazquez, V. Franco, A. Conde, L.F. Kiss, Influence of Cu addition on the magnetic and magnetotransport properties of HITPERM-type alloys, Journal of Magnetism and Magnetic Materials, 262 (2003) 170-173.
[25] K. Nakamura, T. Watanabe, K. Katayama, SOME ASPECTS OF NONISOTHERMAL CRYSTALLIZATION OF POLYMER .1. RELATIONSHIP BETWEEN CRYSTALLIZATION TEMPERATURE, CRYSTALLINITY, AND COOLING CONDITIONS, Journal of Applied Polymer Science, 16 (1972) 1077-&.
[26] J.S. Blazquez, V. Franco, C.F. Conde, A. Conde, L.F. Kiss, Thermal and microstructural dependence of the initial permeability of Co60Fe18Nb6(B,Cu)(16) alloys, Journal of Alloys and Compounds, 431 (2007) 100-106.
[27] J.S. Blazquez, C.F. Conde, A. Conde, T. Kulik, A direct extension of the Avrami equation to describe the non-isothermal crystallization of Al-base alloys, Journal of Alloys and Compounds, 434 (2007) 187-189.
[28] H. Benaini, J.S. Blazquez, C.F. Conde, A. Conde, Kinetic and microstructural studies on the devitrification of Fe60-xCo18MnxNb6B16 amorphous alloys, Journal of Alloys and Compounds, 454 (2008) 156-163.
[29] Z.B. Zhou, M.J. Lai, B. Tang, H.C. Kou, H. Chang, Z.S. Zhu, J.S. Li, L.A. Zhou, Non-isothermal phase transformation kinetics of omega phase in TB-13 titanium alloys, Materials Science and Engineering a-Structural Materials Properties Microstructure and Processing, 527 (2010) 5100-5104.
[30] L.H. Kong, Y.L. Gao, T.T. Song, G. Wang, Q.J. Zhai, Non-isothermal crystallization kinetics of FeZrB amorphous alloy, Thermochimica Acta, 522 (2011) 166-172.
[31] E.S. Lee, Y.G. Kim, A TRANSFORMATION KINETIC-MODEL AND ITS APPLICATION TO CU-ZN-AL SHAPE MEMORY ALLOYS .1. ISOTHERMAL CONDITIONS, Acta Metallurgica Et Materialia, 38 (1990) 1669-1676.
[32] M.J. Starink, On the meaning of the impingement parameter in kinetic equations for nucleation and growth reactions, Journal of Materials Science, 36 (2001) 4433-4441.

Journal of Alloys and Compounds, 544 (2012) 73-81

http://dx.doi.org/10.1016/j.jallcom.2012.08.002

[33] H.E. Kissinger, REACTION KINETICS IN DIFFERENTIAL THERMAL ANALYSIS, Analytical Chemistry, 29 (1957) 1702-1706.
[34] M.J. Starink, Kinetic equations for diffusion-controlled precipitation reactions, Journal of Materials Science, 32 (1997) 4061-4070.
[35] Y.Q. Gao, W. Wang, ON THE ACTIVATION-ENERGY OF CRYSTALLIZATION IN METALLIC GLASSES, Journal of Non-Crystalline Solids, 81 (1986) 129-134.
[36] J.S. Blazquez, M. Millan, C.F. Conde, A. Conde, Nanocrystallization kinetics under instantaneous growth approximation: Experiments and cellular automata simulations, Physica Status Solidi a-Applications and Materials Science, 207 (2010) 1148-1153.
[37] J.S. Blazquez, C.F. Conde, A. Conde, Cellular automata simulations on nanocrystallization processes: From instantaneous growth approximation to limited growth, Journal of Non-Crystalline Solids, 357 (2011) 2833-2839.
[38] J.S. Blazquez, C.F. Conde, A. Conde, Kinetics of nanocrystallization in FeCoNbB(Cu) alloys, Applied Physics a-Materials Science & Processing, 76 (2003) 571-575.
[39] J.M. Borrego, C.F. Conde, A. Conde, M. Stoica, S. Roth, J.M. Greneche, Crystallization behavior and magnetic properties of Cu-containing Fe-Cr-Mo-Ga-P-C-B alloys, Journal of Applied Physics, 100 (2006) 043515.

Journal of Alloys and Compounds, 544 (2012) 73-81

http://dx.doi.org/10.1016/j.jallcom.2012.08.002

Figure captions

Figure 1. a) Values of T_O' as a function of the temperature at which the approximation of Nakamura expression is performed for different values of activation energy. The dashed red line is a linear fitting to the curve corresponding to Q=4 eV. b) Left axis: Comparison between $A(T)$ (symbols) and the proposed approximation $\frac{k'_0}{k_0}(T - \frac{T_p}{2})$ (red line). Right axis: Corresponding dX/dt curve generated using Nakamura kinetic equation at 10 K/min (Q=4 eV; n=4) (black line).

Journal of Alloys and Compounds, 544 (2012) 73-81

http://dx.doi.org/10.1016/j.jallcom.2012.08.002

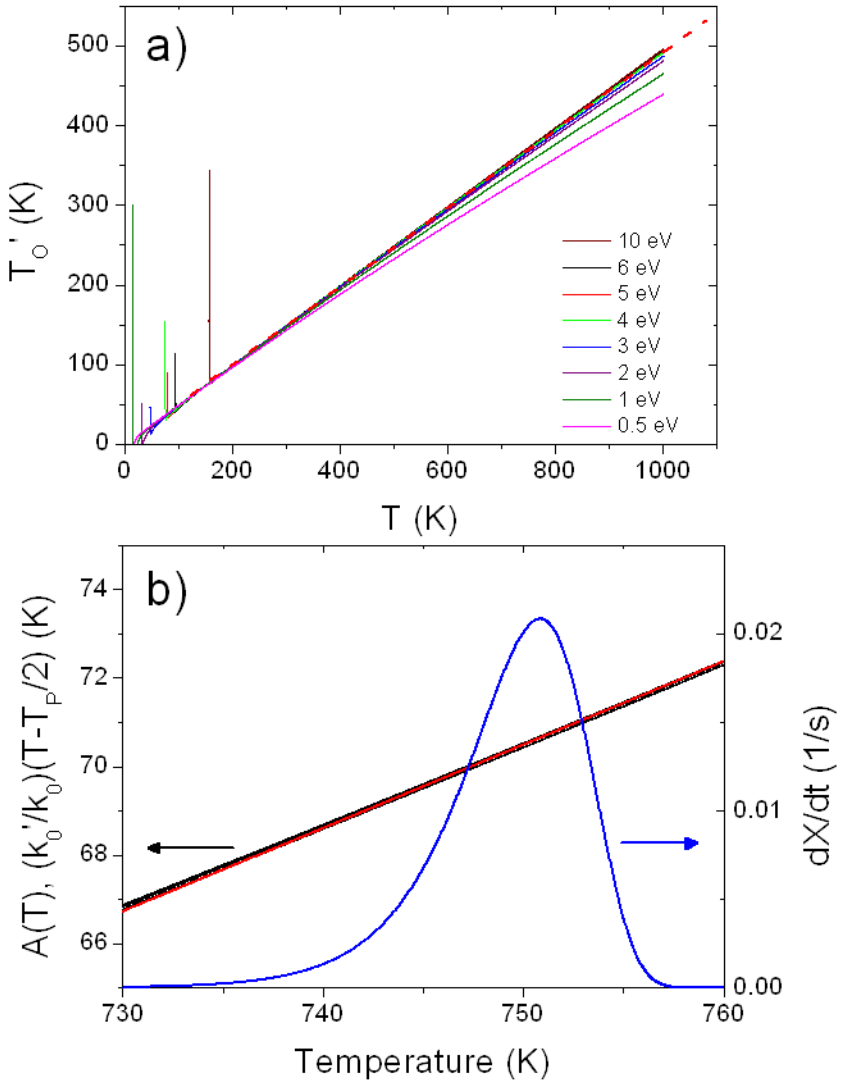

Journal of Alloys and Compounds, 544 (2012) 73-81

http://dx.doi.org/10.1016/j.jallcom.2012.08.002

Figure 2. Avrami exponent obtained applying Eq. (11) (using several values of T_O') to the data generated using Nakamura kinetic equation (inset) at different heating rates (Q=4 eV; n=1; k_0=10^{25} s^{-1}). The inset shows the corresponding dX/dt curve.

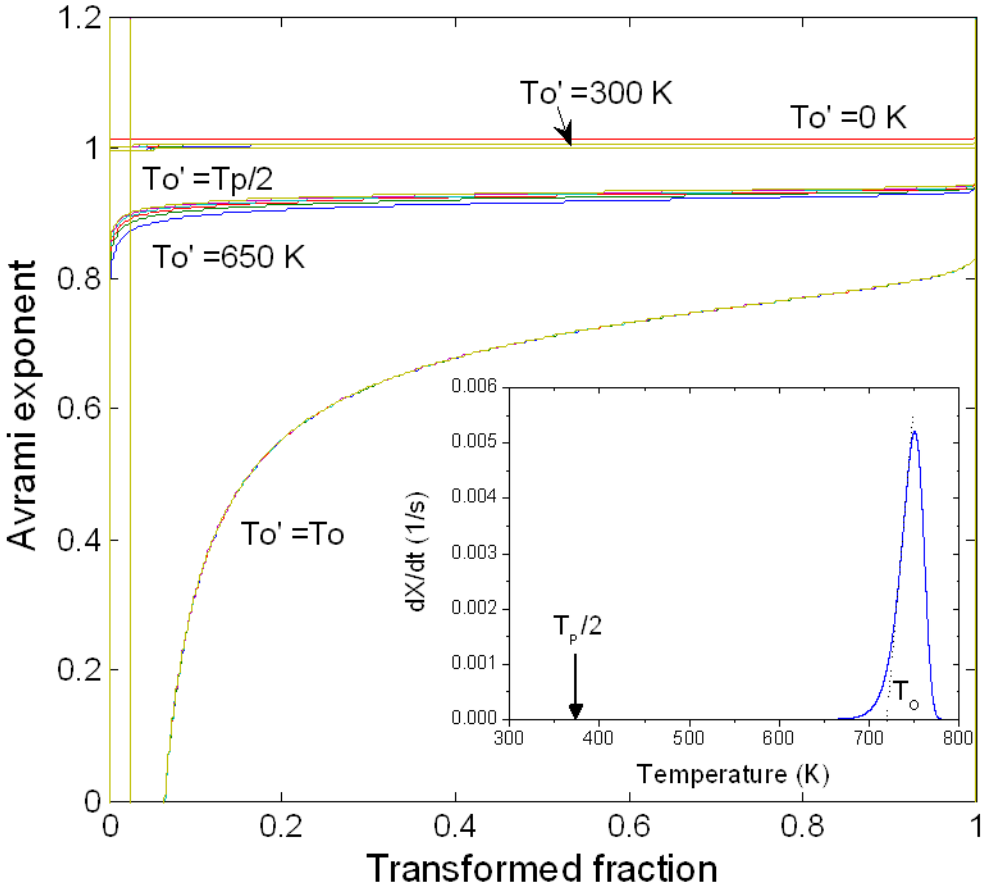

Journal of Alloys and Compounds, 544 (2012) 73-81

http://dx.doi.org/10.1016/j.jallcom.2012.08.002

Figure 3. a) Generated DSC peaks using Eq. (12) with Q_1=4 eV, n_1=2.5, k_{10}=10^{25} s^{-1}; Q_2=3 eV, n_2=1.5, k_{20}=10^{18} s^{-1} (Example shown for f=0.5 and β=10 and 60 K/min). b) Corresponding Avrami exponents for the indicated values of f and β=10 K/min (dark blue), 20 K/min (green), 30 K/min (red), 40 K/min (light blue), 50 K/min (purple) and 60 K/min (dark yellow).

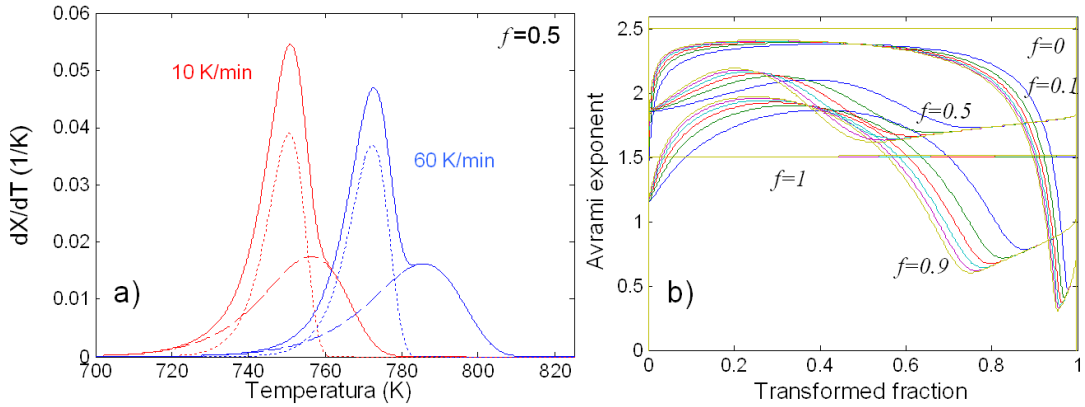

Journal of Alloys and Compounds, 544 (2012) 73-81

http://dx.doi.org/10.1016/j.jallcom.2012.08.002

Figure 4. Activation energies obtained from Kissinger analysis on generated curves using Eq. (12) with the parameters shown in the inset.

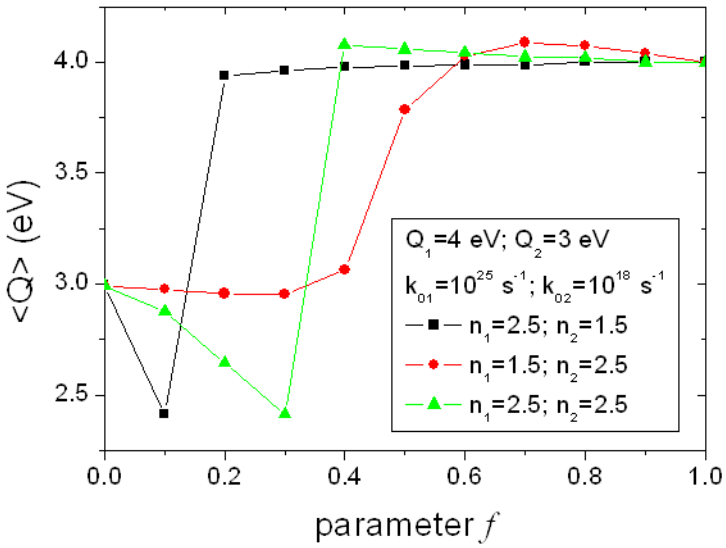

Journal of Alloys and Compounds, 544 (2012) 73-81

http://dx.doi.org/10.1016/j.jallcom.2012.08.002

Figure 5. Left column: Generated DSC peaks using Eq. (13) for two different heating rates and: a) Q_1=4 eV, n_1=1.5, k_{10}=10^{25} s^{-1}; Q_2=3 eV, n_2=2.5, k_{20}=10^{18} s^{-1}; b) Q_1=4 eV, n_1=4, k_{10}=10^{25} s^{-1}; Q_2=3 eV, n_2=1.5, k_{20}=$2\cdot10^{18}$ s^{-1}; c) Q_1=4 eV, n_1=4, k_{10}=10^{25} s^{-1}; Q_2=4 eV, n_2=1.5, k_{20}=10^{25} s^{-1}. Right column: d), e) and f) show the Avrami exponents corresponding to cases a), b) and c), respectively. Different colors correspond to different β as in Fig. 3. Arrows indicate the evolution of the curves as β increases from 10 to 60 K/min when applicable.

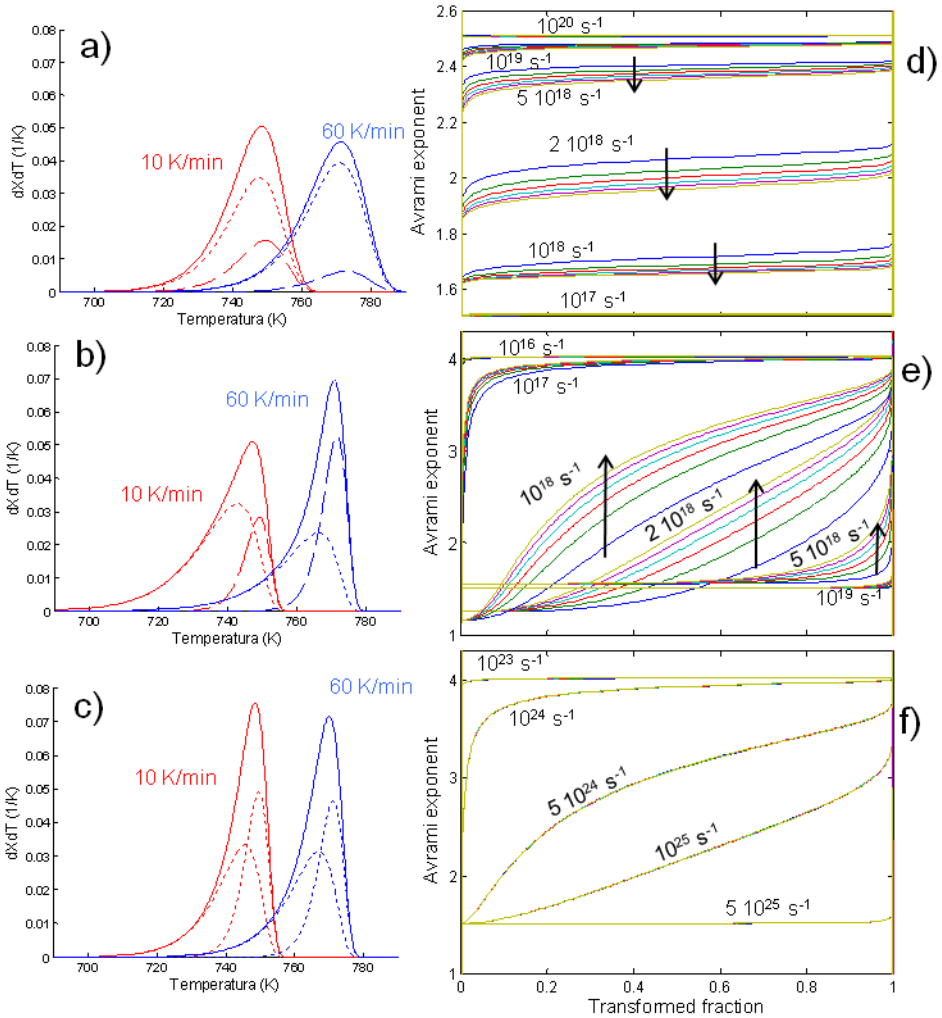

Journal of Alloys and Compounds, 544 (2012) 73-81

http://dx.doi.org/10.1016/j.jallcom.2012.08.002

Figure 6. Application of Eq. (11) to experimental data of $Fe_{60}Co_{18}Nb_6B_{16}$ using different values of T_O'. The inset shows the corresponding DSC curve at 10 K/min.

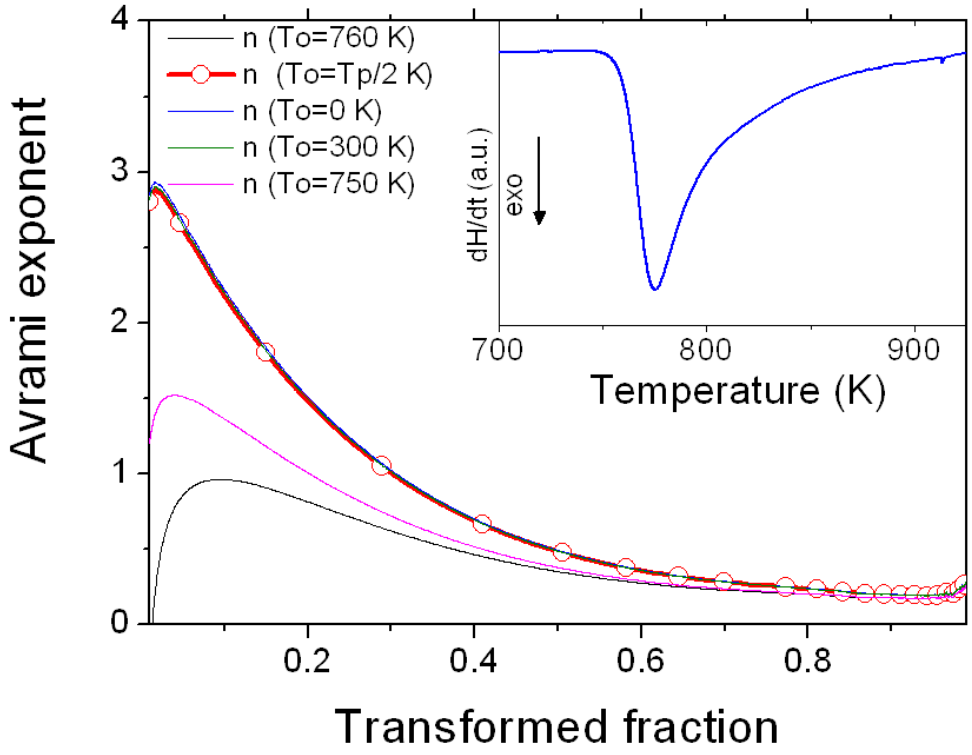

Journal of Alloys and Compounds, 544 (2012) 73-81

http://dx.doi.org/10.1016/j.jallcom.2012.08.002

Figure 7. Left: TEM image of nanocrystallized $Fe_{60}Co_{18}Nb_6B_{16}$ sample. Right: HRTEM image showing a detailed view of an agglomerate formed in this alloy.

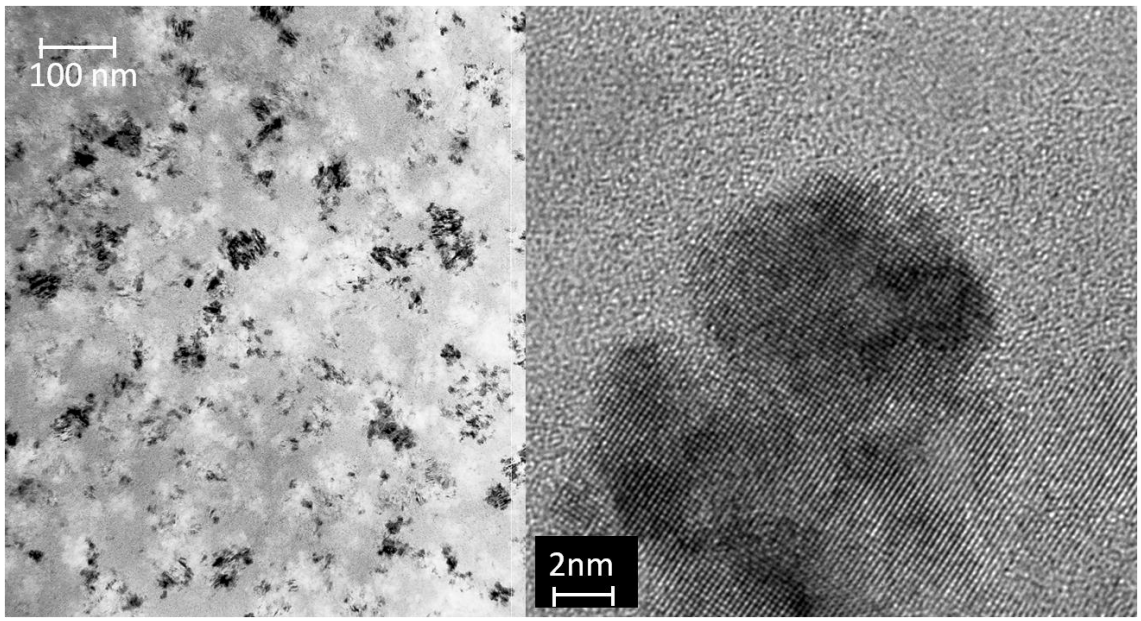

Journal of Alloys and Compounds, 544 (2012) 73-81

http://dx.doi.org/10.1016/j.jallcom.2012.08.002

Figure 8. a) Linear fitting corresponding to Eq. (16). b) Linear fitting corresponding to Eq. (17).

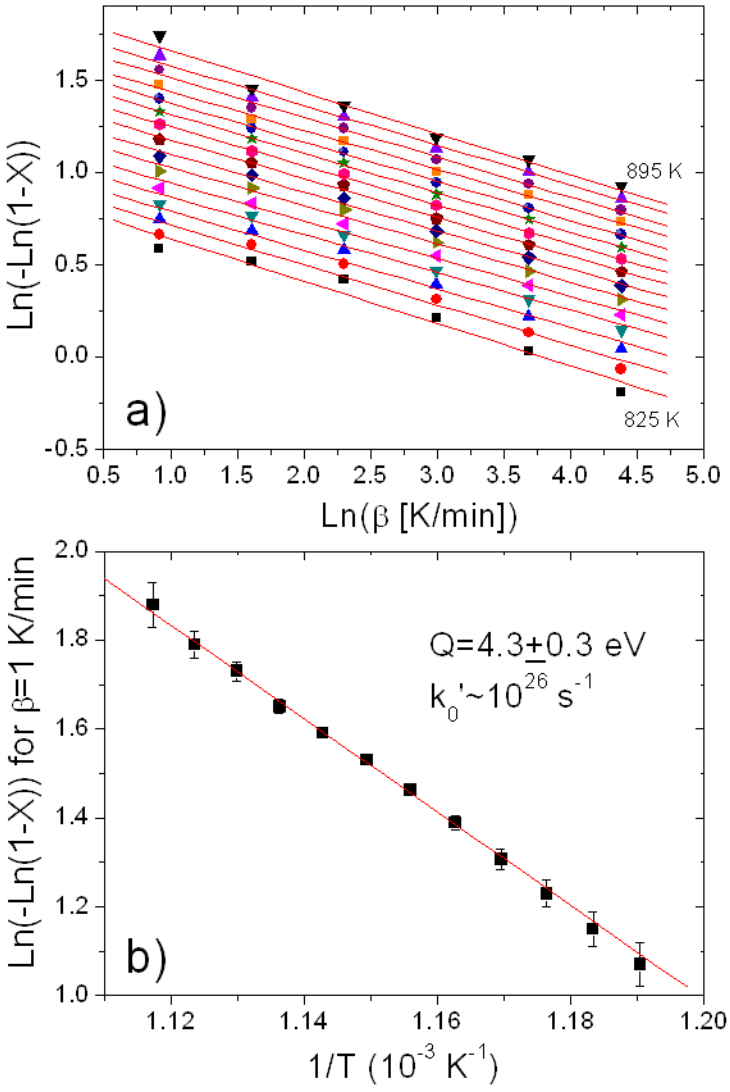

Journal of Alloys and Compounds, 544 (2012) 73-81

http://dx.doi.org/10.1016/j.jallcom.2012.08.002

Figure 9. a) DSC scans of as-cast $Fe_{65.5}Cr_{4-x}Mo_{4-y}Cu_{x+y}Ga_4P_{12}C_5B_{5.5}$ alloys at different heating rates. b) Application of Eq. (11) to experimental data of $Fe_{65.5}Cr_{4-x}Mo_{4-y}Cu_{x+y}Ga_4P_{12}C_5B_{5.5}$ alloys using $T_O' = T_p/2$.

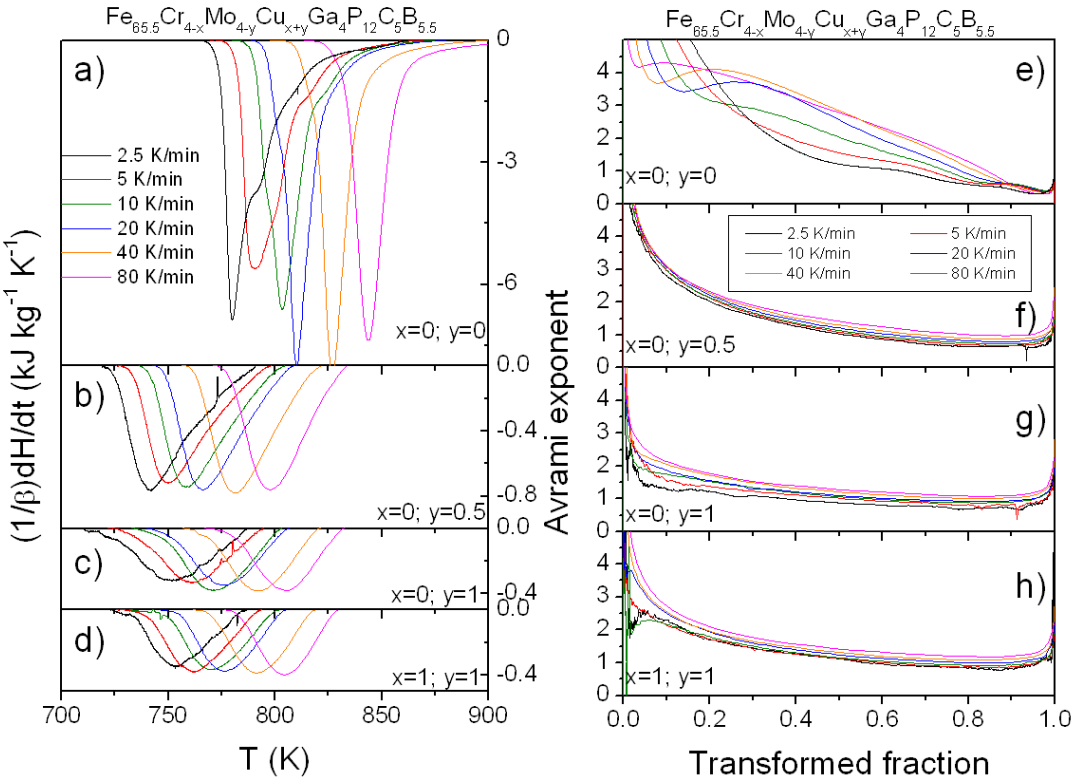

Journal of Alloys and Compounds, 544 (2012) 73-81

http://dx.doi.org/10.1016/j.jallcom.2012.08.002

Figure 10. TEM images of as-cast and nanocrystallized samples of $Fe_{65.5}Cr_{4-x}Mo_{4-y}Cu_{x+y}Ga_4P_{12}C_5B_{5.5}$ alloys. The grain size histograms of nanocrystallized samples are also shown.